ACS OMEGA

http://pubs.acs.org/journal/acsodf

Article

Hydrogen Bond Patterns of Dipyridone and Bis(Hydroxypyridinium) Cations

Midhun Mohan, Mohamed Essalhi, Sarah Zaye, Love Karan Rana, Thierry Maris, and Adam Duong*

Cite This: *ACS Omega* 2021, 6, 35649−35656

Read Online

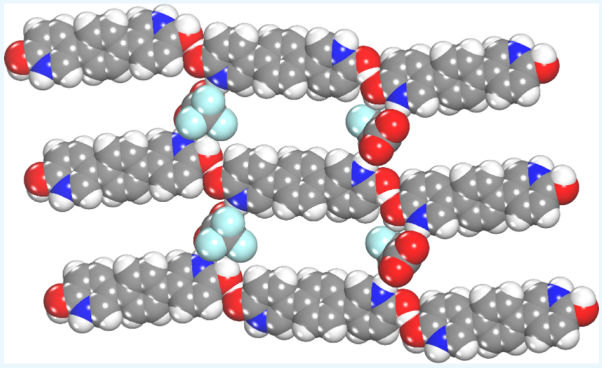

ABSTRACT: Dipyridonyl-substituted derivatives **2−4** of benzene, pyridine, and pyrazine, respectively, were synthesized to examine the ability of 2-pyridone and its protonated species to direct the self-assembly by hydrogen bonding. Structural analysis by single-crystal X-ray diffraction (SCXRD) of **2** and **4** in trifluoroacetic acid demonstrated that salts are formed as a result of the transfer of protons from the acid to the base (organic species) to generate a bis(hydroxypyridinium) dication. However, if no proton transfer takes place like in the case of crystals of **3** grown from DMSO/H_2O, the self-assembly is mainly directed by the typical $\mathbf{R}_2^2(8)$ hydrogen bond motif of 2-pyridone. These results indicate that the process of converting a neutral 2-pyridonyl group into a hydroxypyridinium cation makes structure prediction difficult. Consequently, examination of proton transfer and assembly of dipyridone and its protonated species are of interest. In combination with SCXRD, Hirshfeld surface analysis (HSA) was also used to have a better understanding on the nature of intermolecular interactions within crystal structures of **2−4**. The large number of F···H/H···F, H···O/O···H, H···H, and H···C/C···H contacts revealed by HSA indicates that hydrogen bonding and van der Waals interactions mainly contribute to crystal packing.

■ INTRODUCTION

Since hydrogen bonds were discovered, efforts to characterize and understand their use to direct the molecular organization have flourished.[1,2] Among other interactions, hydrogen bonding has played a key role in the design of supramolecular chemistry. The directionality and reversible character of the hydrogen bonds made this intermolecular interaction extremely useful to tailor-made architectures.[3] Therefore, hydrogen bonds are important for the development of fundamental and applied fields. They are the most commonly used intermolecular interactions to design ordered bulk materials.[4,5] Single-crystal X-ray diffraction (SCXRD) is one of the main characterization techniques that have been extensively used to elucidate the hydrogen bonding patterns of various compounds which incorporate one or multiples sticky sites such as hydroxy (−OH), carboxylic (−COOH), diaminotriazinyl (DAT), pyridonyl groups, etc.[6−10] In chemistry, the strategy that uses non-covalent interactions to direct the molecular organization is the concept of crystal engineering.[11]

Among the various sticky sites by hydrogen bonds, the 2-pyridone group has been the least used to produce crystalline materials.[12,13] 2-Pyridone exists as tautomers in which the proton can be attached to nitrogen or to oxygen to form lactam and 2-hydroxypyridine, respectively.[14−16] So far, to the best of our knowledge, only 14 structures are reported on organic crystals containing two to four 2-pyridone groups.[13,17−21] Their crystal structures reveal mainly hydrogen bonds with the $\mathbf{R}_2^2(6)$ synthon, and only a few exhibit a **C(3)** pattern (Chart 1a).[22] Under acidic conditions, a hydroxypyridinium cation species (Chart 1b) can be formed by protonation of a pyridone, which results in different hydrogen bonding patterns as compared to the parent one, thus making the structural prediction more complicated. Therefore, to better understand the assembly of 2-pyridone and its protonated derivatives, we focused our work on the design, synthesis, and characterization of novel dipyridone compounds **2−4** (Chart 1c). They consist of 1,4-dipyridone-substituted derivatives of benzene, pyridine, and pyrazine. These compounds are interesting owing to their abilities to self-assemble by hydrogen bonds or to coordinate metal ions to form fascinating networks.[12,23−25] The incorporation of the spacers such as phenyl, pyridyl, and pyrazinyl can facilitate the formation of longer and functionalized links for the synthesis of novel metal−organic frame-

Received: October 6, 2021
Accepted: November 3, 2021
Published: December 14, 2021

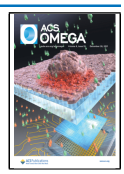

Chart 1. (a) Typical Hydrogen Bonding Synthon of the 2-Pyridone Group and (b,c) Molecular Structures of the Hydroxypyridinium Cation, 1−4 and 2′−4′, Respectively

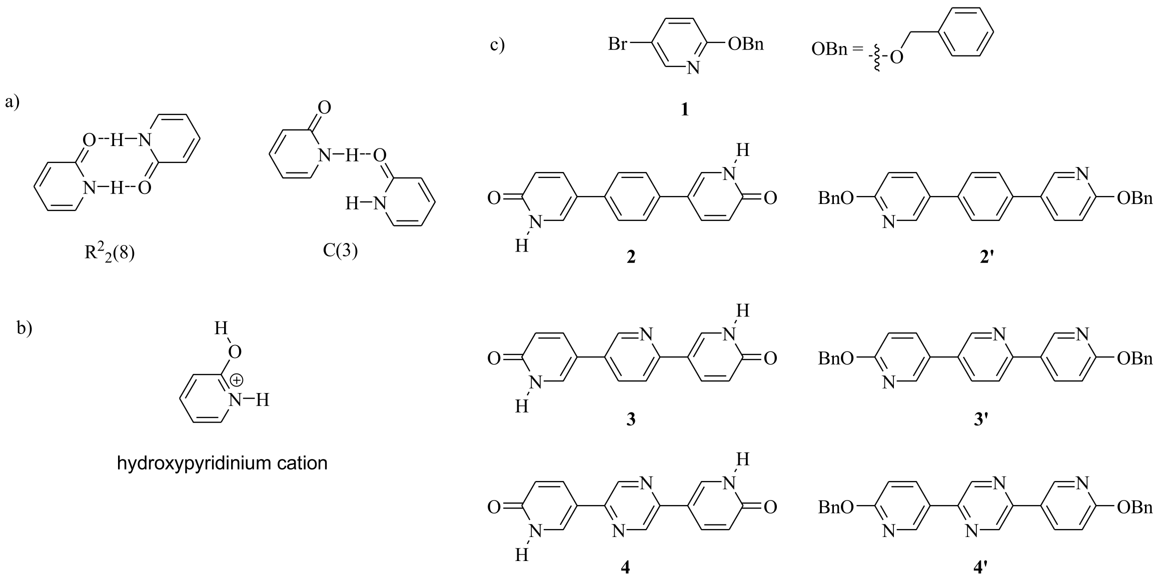

Scheme 1. Synthesis of 2′−4′ and 2−4

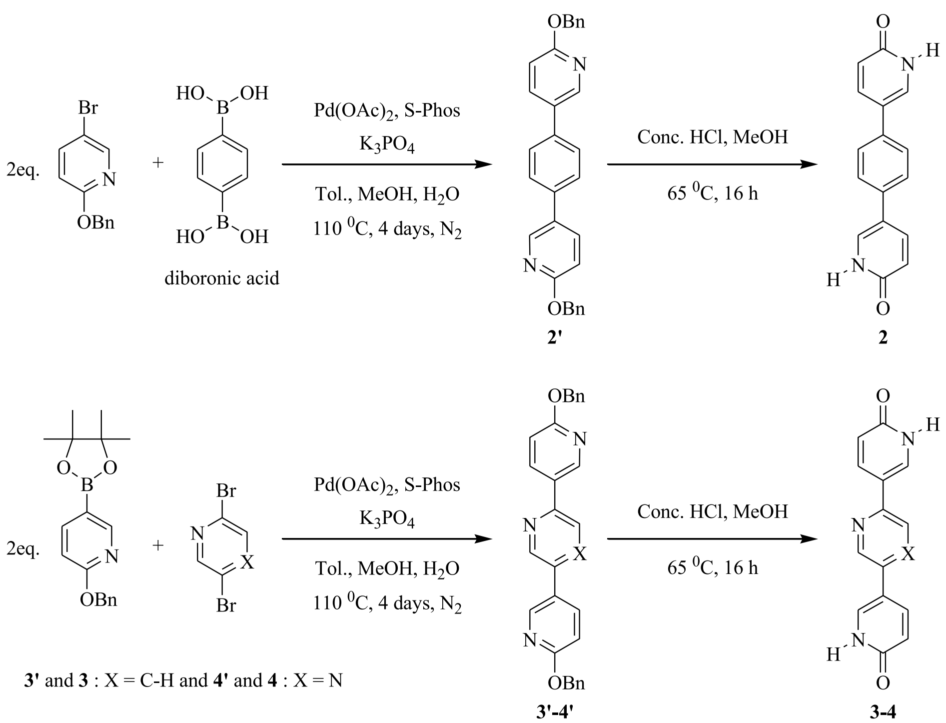

works (MOFs) with intrinsic properties. Herein, we studied the aggregations via hydrogen bonds of **2−4** and the protonated species using SCXRD and Hirshfeld surface analysis (HSA).

■ RESULTS AND DISCUSSION

Syntheses of Compounds 1, 2−4, and 2′−4′. 2-(Benzyloxy)-5-bromopyridine **1** was prepared following methods reported previously.[26] Compounds **2′−4′** were synthesized with yield ranging from 80 to 90% by Suzuki−Miyaura coupling reaction.[27,28] Deprotection of the benzyl group under acidic conditions gives **2−4** in quantitative yield (Scheme 1).

Structures of **2−4** and **2′−4′** were determined using electrospray ionization mass spectrometry (ESI-MS) and infrared (IR) and ^{1}H and ^{13}C nuclear magnetic resonance (NMR) spectroscopies. IR spectra of **2′−4′** show characteristic absorption bands at 3042−3030 and 1602−1601 cm^{-1}, which correspond to the C−H and C═C stretching vibrations, respectively. The bands at 1357, 1344, and 1395 cm^{-1} for **2′−4′**, respectively, are assigned to the aromatic C−N stretching vibrations. The characteristic C−O stretching vibrations in **2′−4′** are evident at 1286, 1283, and 1269 cm^{-1}, respectively. Also, other significant bands are observed at 1010, 1006, and 1021 cm^{-1} for **2′−4′**, which are attributed to the C═C bending vibrations. Comparatively, in **2−4**, characteristic aromatic C−

https://doi.org/10.1021/acsomega.1c05561
ACS Omega 2021, 6, 35649−35656

H stretching vibrations are observed at 3271, 3271, and 3046 cm^{-1}, respectively. The bands at 2829, 2830, and 2690 cm^{-1} are assigned to N−H stretching vibrations. The C═O stretching vibrations are assigned at 1645, 1650, and 1685 cm^{-1}, respectively, along with C═C stretching vibrations at 1645−1614 cm^{-1}, C−N stretching in the range of 1342−1310 cm^{-1}, and C═C bending vibrations at 996−989 cm^{-1} for **2**−**4**. The thermal analyses of **2**−**4** were conducted within the temperature range of 25−800 °C. All compounds are stable up to ∼350, 370, and 415 °C, respectively, above which the materials start to decompose. The initial 8% weight loss in **2** can be attributed to the surface moisture, and then, the weight loss of 67% signifies the phase change followed by the decomposition. For **3**, the first step with a 9% weight loss occurs as a result of the surface-adsorbed moisture and other trace amounts of solvents used while purification. This is followed by a 46.5% weight loss corresponding to the phase change and decomposition. In the case of **4**, a 51% weight loss at 415 °C is assigned to the phase change and decomposition points. SCXRD is performed to reveal the molecular organization by hydrogen bonds of **2**−**4**.

Crystal Structures. *Structure of 5-(4-(1,6-Dihydro-6-oxopyridin-3-yl)phenyl)pyridin-2(1H)-one* ***2*** *as a Trifluoroacetate Salt.* Crystals of **2** grown from trifluoroacetic acid (TFA)/$CHCl_3$ proved to belong to the triclinic space group $P\bar{1}$ and have the composition of $(\mathbf{2}H_2)^{2+}$ • $2(CF_3COO)^-$. Views of the structures are shown in Figure 1. Additional crystallographic data are given in Table 1. In the crystal structure, the organic moiety is diprotonated to give a bis(hydroxypyridinium) species $(\mathbf{2}H_2)^{2+}$ and trifluoroacetate $(CF_3COO)^-$ anions balance the positive charge. The molecular structure of $(\mathbf{2}H_2)^{2+}$ shows an identical twist angle

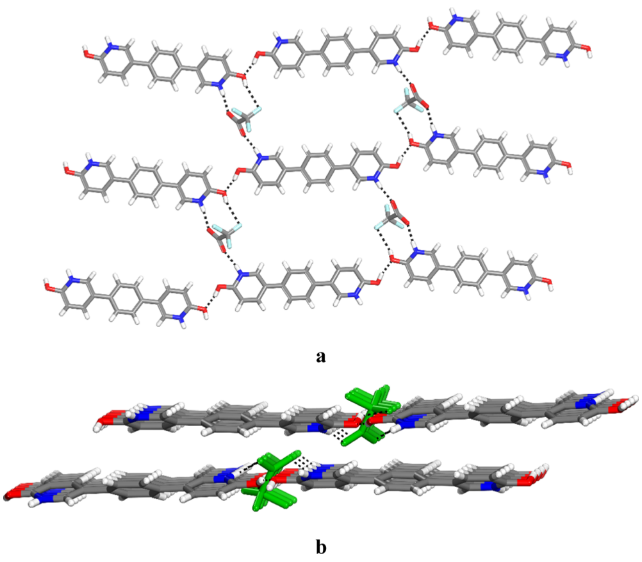

Figure 1. Representation of the crystal structure of the trifluoroacetate salt of 5-(4-(1,6-dihydro-6-oxopyridin-3-yl)phenyl)pyridin-2(1*H*)-one **2** grown from TFA/$CHCl_3$. (a) Cationic $(\mathbf{2}H_2)^{2+}$ are linked to form chains by O−H···O hydrogen bonds, and chains are further interconnected by N−H···O and O−H···F involving bridging trifluoroacetate anions to generate a layer. (b) View along the *b*-axis showing the stacking of layers maintained together by hydrogen bonding involving bridging of $(CF_3COO)^-$. For clarity, $(CF_3COO)^-$ molecules are marked in green. Hydrogen bonds are represented by broken lines. C, gray; O, red; N, blue; H, white; and F, cyan.

Table 1. Crystallographic Data for 2−4

	2	3	4
formula	$C_{16}H_{14}N_2O_2^{2+}$· $2CF_3COO^-$	$C_{15}H_{11}N_3O_2$· $2H_2O$	$C_{14}H_{12}N_4O_2^{2+}$· $2CF_3COO^-$
Mr	492.33	301.30	494.32
crystal system	triclinic	monoclinic	monoclinic
space group	$P\bar{1}$	$P2_1/n$	$P2_1/n$
a (Å)	10.3440(9)	13.2786(15)	8.5865(3)
b (Å)	10.4190(11)	3.7845(5)	11.2015(4)
c (Å)	10.5800(11)	14.1350(17)	20.1697(7)
α (deg)	92.229(7)	90	90
β (deg)	102.919(6)	104.613(7)	99.146(2)
γ (deg)	103.078(6)	90	90
V (Å^3)	1077.74(19)	687.35(15)	1915.25(12)
Z	2	2	4
ρ_{calcd} (g cm^{-3})	1.517	1.456	1.714
T (K)	100	298(2)	150
radiation	Cu Kα	Cu Kα	Ga Kα
λ (Å)	1.54178	1.54178	1.34139
μ (mm^{-1})	1.293	0.900	0.948
F(000)	500	316	1000
no. measured reflections	16809	8690	24671
no. independent reflections	3962	1344	3925
no. obsd. reflections $I > 2\sigma(I)$	2916	1144	2910
Nb Params	437	110	437
R_1, $I > 2\sigma$ (%)	0.0661	0.0654	0.0664
R_1, all data (%)	0.0798	0.0735	0.0885
ωR_2, $I > 2\sigma$(I) (%)	0.2027	0.1851	0.1721
ωR_2, all data (%)	0.2128	0.1995	0.1901
GoF	1.086	1.093	1.070

for both hydroxypyridinium groups with the phenyl ring (29.24 and 31.62° for the two molecules in the asymmetric unit, respectively). The two N−H and O−H of the hydroxypyridinium are *trans*-oriented, and all C−N and C−C bonds are normal (average bond lengths d_{C-N} = 1.358 Å, d_{C-O} = 1.269 Å, and d_{C-C} = 1.394 Å).[8,13] Cationic units $(\mathbf{2}H_2)^{2+}$ are linked according to $\mathbf{D}_1^1(\mathbf{2})$ motifs (O−H···O (2.431 Å)) to form chains which are further interconnected by another $\mathbf{D}_1^1(\mathbf{2})$ motif (N−H···O_{TFA} (2.786 Å)) to generate a new binary graph set $\mathbf{R}_6^6(42)$ in a layer (Figure 1a).[22] It is not worthy that hydrogen bonds between the free −OH group of the hydroxypyridinium and the closest fluorine atom (O−H···F (2.471 Å)) reinforce the 2D network. Layers are then joined by multiple hydrogen bonding involving trifluoroacetate molecules to produce the three-dimensional (3D) network (Figure 1b). Selected hydrogen bonds and angles are given in Tables S1−S4.

A non-symmetric compound of **3** has been designed by replacing one C−H with the N atom in the spacer benzene ring of **2**. Compound **3** was synthesized, dissolved in TFA, and subjected to several crystallization techniques to form single crystals for XRD analysis. Despite all the attempts made, especially in TFA, none are successful to produce crystals. However, single crystals of **3** could be grown from DMSO/EtOH.

Structure of 5-(5-(1,6-Dihydro-6-oxopyridin-3-yl)pyridin-2-yl)pyridin-2(1H)-one ***3***. Crystals of **3** grown from DMSO/EtOH proved to belong to the monoclinic space group $P2_1/n$ and have the composition $\mathbf{3}\cdot 2(H_2O)$. Figure 2 shows views of

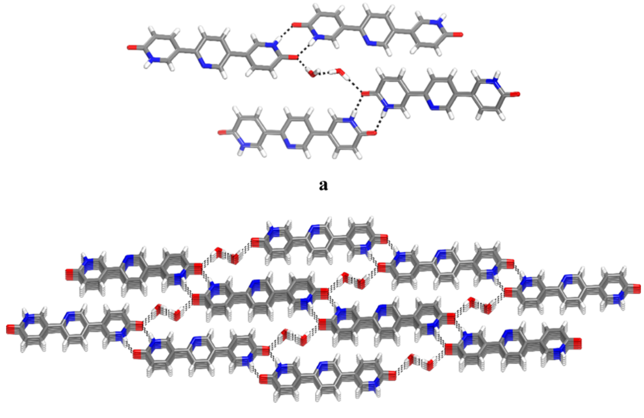

a

b

Figure 2. Views of the structure of 5-(5-(1,6-dihydro-6-oxopyridin-3-yl)pyridin-2-yl)pyridin-2(1*H*)-one **3**. (a) Zigzag chains formed by cyclic N−H···O hydrogen bonds and their interconnection by bridging of water molecules. (b) View showing the 3D network produced by hydrogen bonds and $\pi-\pi$ stacking. Hydrogen bonds are represented by broken lines. C, gray; O, red; N, blue; H, white.

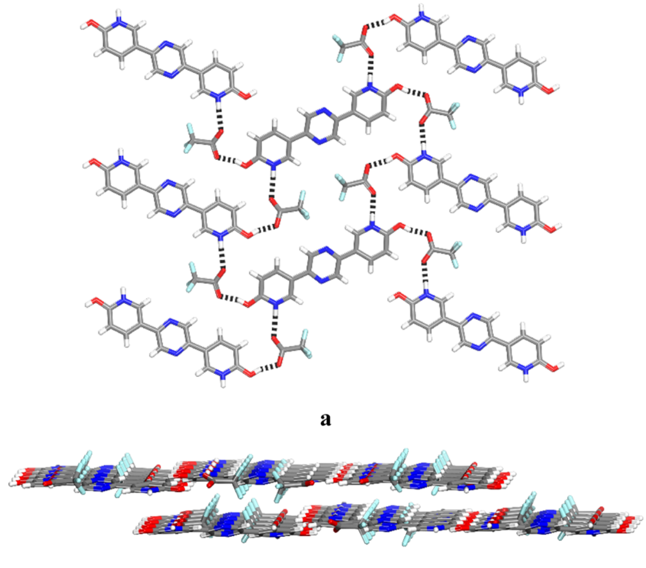

a

b

Figure 3. Views of the structure of 5-(5-(1,6-dihydro-6-oxopyridin-3-yl)pyridin-3-yl)pyridin-2(1H)-one **4** grown from TFA/H_2O. (a) View showing a layer formed by hydrogen bonds between $(\mathbf{4}H_2)^{2+}$ and trifluoroacetate. (b) View along the *b*-axis showing packing of layers. Hydrogen bonds are represented by broken lines. C, gray; O, red; N, blue; H, white; and F, cyan.

the structure of **3**, and other crystallographic data are provided in Table 1. The twist angle between pyridonyl and pyridyl rings (26.10°) is slightly smaller compared with **2**. All C−N, C−O, and C−C bonds are normal (average bond lengths d_{C-N} = 1.359 Å, d_{C-O} = 1.256 Å and d_{C-C} = 1.630 Å).[8,13] In the structure, organic species self-assemble by N−H···O hydrogen bonds (2.790 Å) according to the $\mathbf{R}_2^2(8)$ motif to form a zigzag chain (Figure 2b).[22] Chains are then interconnected by multiple hydrogen bonds involving bridging of water molecules to produce complex graph sets $\mathbf{R}_8^8(42)$ in a 3D network.[22] The network is also strengthened by $\pi-\pi$ stacking (3.784 Å) of heterocycles (Figure 2b). It is noteworthy that the nitrogen atom of the pyridyl ring does not participate in any hydrogen bonding. Summary of hydrogen bonds and angles is provided in Tables S5 and S6.

The replacement from C−H to the N atom does not affect the molecular conformation of molecule **3**. The only slight difference is the twisted angles between pyridonyl and pyridyl rings. The crystallization with a non-acidic medium gives a self-assembly of **3** with a known hydrogen bonding motif of 2-pyridone (Chart 1). The behavior of the 2-pyridonyl group in TFA prompted us to examine the corresponding pyrazine **4**, in which two C−H in the spacer benzene ring have been replaced with the N atom as compared with **2**.

*Structure of 5-(5-(1,6-Dihydro-6-oxopyridin-3-yl)pyrazin-2-yl)pyridin-2(1H)-one **4** as a Trifluoroacetate Salt.* Crystals of **4** grown from TFA/H_2O proved to belong to the monoclinic space group $P2_1/n$ and have the composition of $(\mathbf{4}H_2)^{2+} \bullet 2(CF_3COO)^-$. SCXRD of **4** reveals the presence of an organic species diprotonated forming a dication $(\mathbf{4}H_2)^{2+}$ like for **2**. Both 2-pyridonyl groups are protonated to give a bis(hydroxypyridinium) species. In the structure, the molecule $(\mathbf{4}H_2)^{2+}$ is nearly planar with pyrazinyl and hydroxypyridinium ring twisted angles of 9.10 and 4.96°. Again, the N−H and O−H groups are *trans*-oriented. Dicationic $(\mathbf{4}H_2)^{2+}$ species are interconnected involving bridging of trifluoroacetate anions according to unitary graph sets $\mathbf{D}_1^1(\mathbf{2})$ (N−H···O (2.798 Å, 2.699 Å) and O−H···O (2.455 Å, 2.480 Å)) to produce a ring with graph set symbol $\boldsymbol{R}_8^8(50)$ within a layered structure (Figure 3a).[22] Details of hydrogen bonds and angles are provided in Tables S7−S10. Layers are further $\pi-\pi$ stacking (3.721 Å) to produce the thickness of crystals (Figure 3b). It is noteworthy that here again, all C−N, C−O, and C−C bonds are normal (average bond lengths d_{C-N} = 1.174 Å, d_{C-O} = 1.302 Å, and d_{C-C} = 1.400 Å).[8,13]

Hirshfeld Surface Analysis. The intermolecular interactions in **2**−**4** have been further examined and visualized by HSA using CrystalExplorer21 software.[29] d_{norm} mapped on HSA (Figure 4) shows short intermolecular contacts as red spots. They are ascribed to O−H···O, N−H···O, and O−H···F hydrogen bonds in **2** and **4** (Figure 4a,c). In the case of **3**, these red spots correspond to O−H···O and N−H···O hydrogen bonds and C−H···O contacts (Figure 4b).

The overall fingerprint plot for **2**−**4** is shown in Figure 5. The most prominent types of contacts in **2** and **4** structures correspond to O···H/H···O (observed as a pair of spikes) and F···H/H···F contacts; they contribute together to 49.3 and 44.5% to the overall surface contacts, respectively, to the overall surface contacts. For **3**, O···H/H···O and H···H contacts contribute to 67% to the overall surface contacts. The fingerprint plot for H···H contacts (11.8% contribution) in **2** has a spike indicating C−H···F contacts (Figure 5a). All compounds present C−H···π interactions characterized by a pair of wings in the fingerprint plot decomposed into C···H/H···C contacts contributing 13.6%, 13.3%, and 8.6% to the HS. The contributions of other contacts to the HS are negligible for all structures.

■ CONCLUSIONS

Although the 2-pyridone group is well known in crystal engineering, only a few organic crystals have shown structures with two or more of this sticky site. Our work illustrated that the tendency of dipyridone to form $\mathbf{R}_2^2(8)$ and $\mathbf{C}(3)$ synthons is not systematic. It is significantly dependent on the conditions of crystallization. In TFA, 2-pyridonyl groups

https://doi.org/10.1021/acsomega.1c05561
ACS Omega 2021, 6, 35649−35656

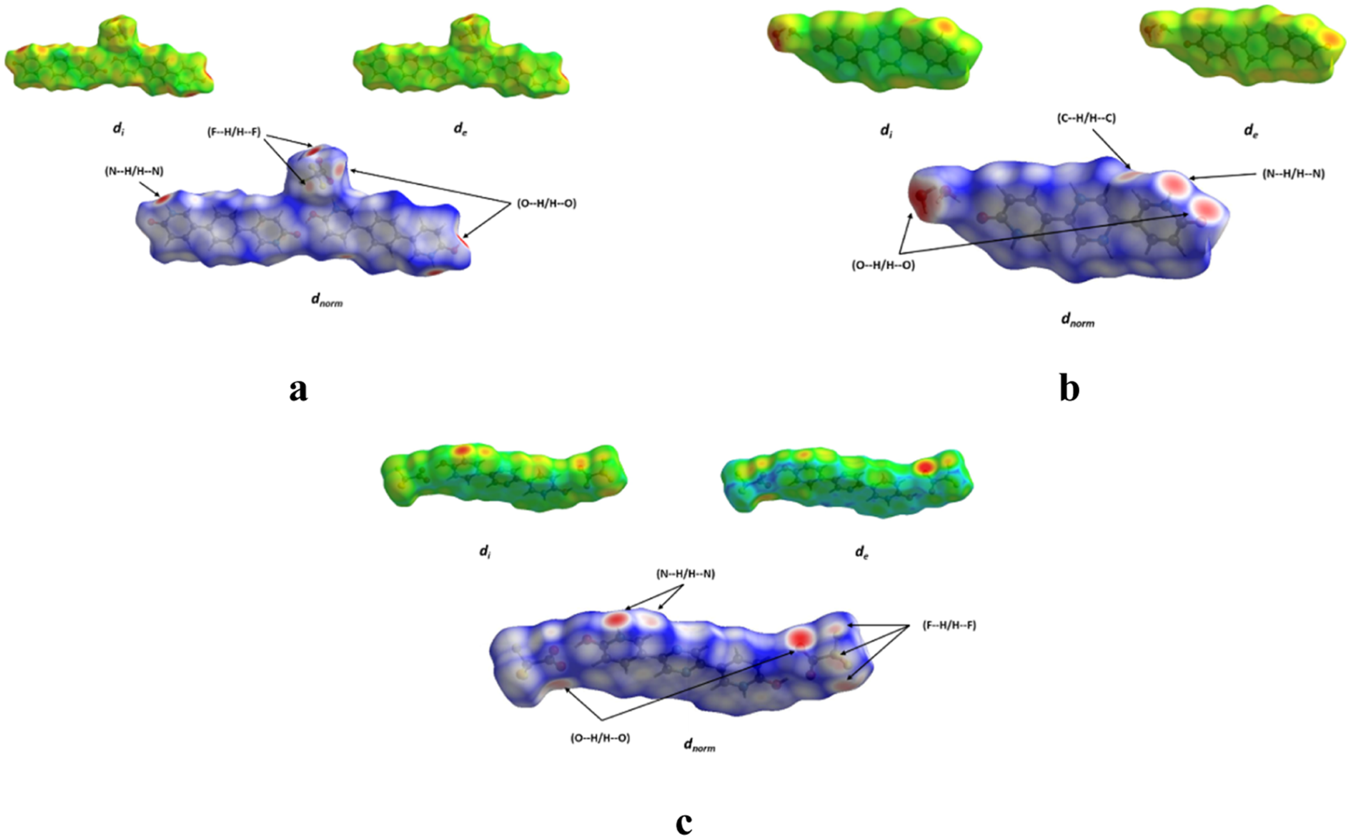

Figure 4. View of the 3D Hirshfeld surface: plotted over d_{norm} in the range of −0,955 to +0.952 a.u. in (a) **2**, (c) **3**, and (e) **4**.

tend to be protonated to generate hydroxypyridinium species. In the structures of **2** and **4** elucidated by SCXRD, the aggregation of molecules is dictated by the hydrogen bonds and the coulombic interactions between anionic and cationic species. In DMSO, the 2-pyridonyl group appears to form mainly the conventional $\mathbf{R}_2^2(8)$ and $\mathbf{C}(3)$ synthons as illustrated by the structure of **3**. By examining the novel structures of dipyridone **2**−**4** described here in the context of crystal engineering, we were able to investigate the assembly of hydroxypyridinium sticky sites obtained by protonation of 2-pyridone. Furthermore, HSA was employed to investigate the intermolecular interactions in **2**−**4**. These data confirmed the constructive contribution of hydrogen bonds in crystal formation. Our work is useful to understand the molecular organization of dipyridone and bis(hydroxypyridinium) compounds that are not fully explored yet in the field of supramolecular chemistry. It should help researchers that are interested to build reliable molecular networks by hydrogen bonds. Our investigation on the synthetic method of dipyridone promises to be useful for scientists who are involved in the design of coordination polymers via the linkage of 2-pyridone with metal ions.

■ EXPERIMENTAL SECTION

Materials. All chemicals were purchased from commercial sources and were used without further purification. All solvents were purchased from Fischer Scientific. Compounds **2′**−**4′** and **2**−**4** were made by the procedures summarized below.

Single-Crystal X-Ray Diffraction. SCXRD data were obtained using a Bruker Smart APEX diffractometer equipped with an Incoatec Microsource (Cu Kα radiation) for compound **2**, a Bruker Venture Metaljet diffractometer (Ga Kα radiation) for compound **3**, and a Bruker AXS D8 Discover (Cu Kα) for compound **4**. The structures were solved by the dual-space method using SHELXT,[30] and non-hydrogen atoms were refined anisotropically with least squares minimization using SHELXL.[31]

Other Analysis Techniques. The IR(ATR) spectra were recorded with a Nicolet iS 10 Smart FT-IR Spectrometer within 600−4000 cm^{-1}. Thermogravimetric analysis was performed using a Diamond Pyris TGA/DTA apparatus from Perkin-Elmer and a Mettler Toledo TGA/DSC1. ^{1}H and ^{13}C NMR were recorded with a Bruker 400 MHZ and 100 MHZ, respectively.

General Method to Prepare 2′−4′. In an oven-dried Schlenk flask, $Pd(OAc)_2$ (0.101 g, 0.15 mmol) and S-Phos (0.118 g, 0.288 mmol) were dissolved in toluene (20 mL) under inert conditions. To this solution were added (i) 2-(benzyloxy)-5-bromopyridine **1** (0.8451 g, 3.2 mmol) and benzene-1,4-diboronic acid (0.27 g, 1.6 mmol), (ii) 2,5-dibromopyridine (0.38 g, 1.6 mmol) and 2-(benzyloxy)-5-(4,4,5,5-tetramethyl-1,3,2-dioxaborolan-2-yl)pyridine (1 g, 3.2 mmol), and (iii) 2,5-dibromopyrizine (0.38 g, 1.6 mmol) and 2-(benzyloxy)-5-(4,4,5,5-tetramethyl-1,3,2-dioxaborolan-2-yl)-pyridine (1 g, 3.2 mmol) to form **2′**−**4′**, respectively. To these mixtures, K_3PO_4 (6.1137 g, 28.8 mmol) in 12 mL of methanol/water (1:1) was added dropwise. The mixtures were heated at 110 °C under nitrogen for 4 days. The reactions were cooled to room temperature and extracted with dichloromethane. The organic layers were dried over magnesium sulfate and filtered, and the solvent was evaporated under reduced pressure. The residues were purified by column chromatography (silica gel, chloroform/hexane 1:2).

https://doi.org/10.1021/acsomega.1c05561
ACS Omega 2021, 6, 35649−35656

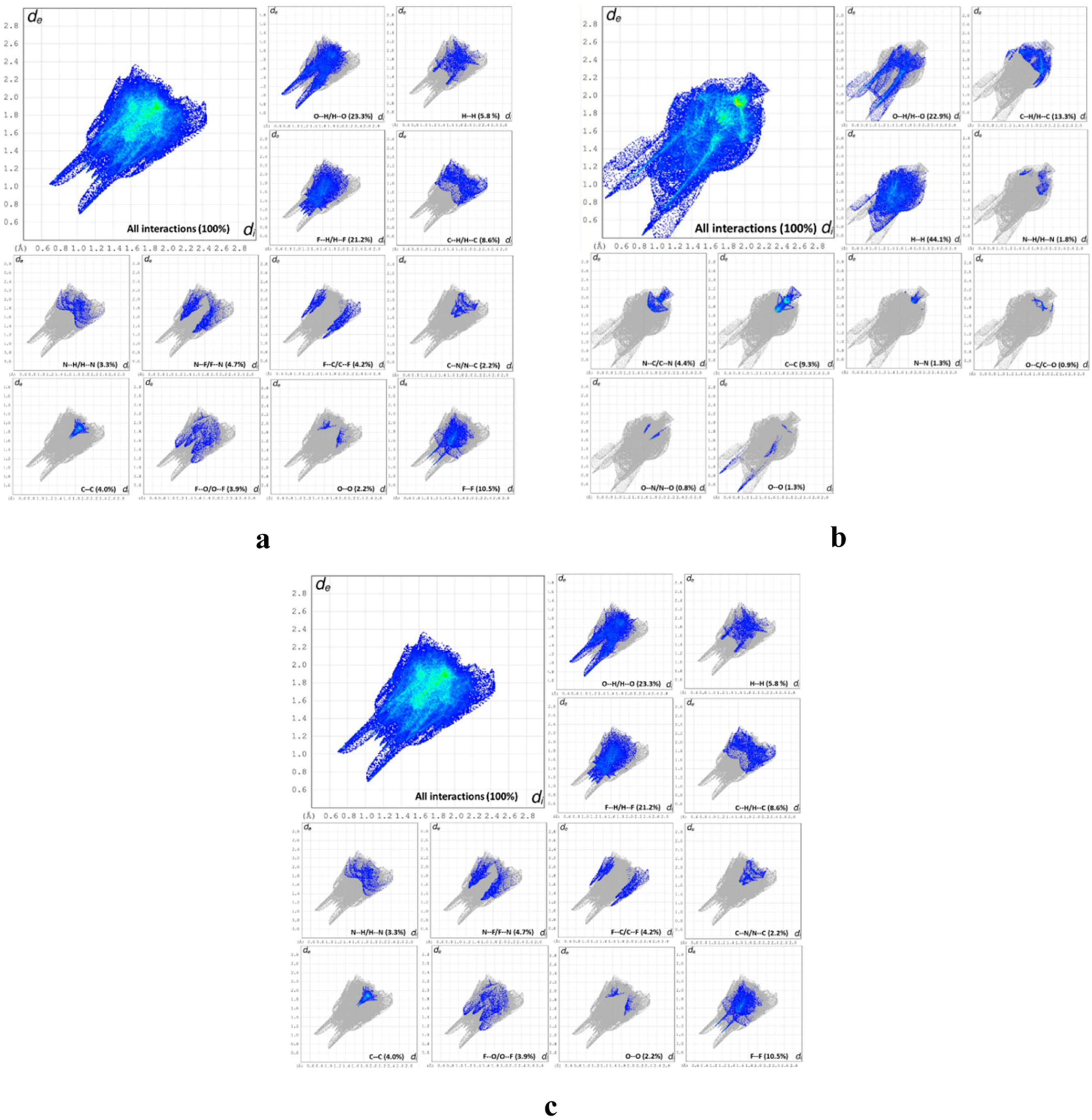

Figure 5. View of the 2D fingerprint plots for all intermolecular contacts in (a) **2**, (b) **3**, and (c) **4**.

*2-(Benzyloxy)-5-(4-(6-(benzyloxy)pyridin-3-yl)phenyl)-pyridine **2**′*. Colorless solid (0.61 g, 1.36 mmol, 85%). mp 211 °C; FTIR ν 3060, 3042, 3022, 2938, 2885, 1301, 1567, 1524, 1475, 1466, 1453, 1425, 1357, 1286, 1243, 1140, 1010, 995, 825, 817, 742, 693 cm^{-1}; ^{1}H NMR (700 MHz, DMSO): δ 8.56 (d, *J* = 2.5 Hz, 1H), 8.11 (dd, *J* = 8.6, 2.6 Hz, 1H), 7.78 (s, 2H), 7.48 (d, *J* = 7.3 Hz, 2H), 7.40 (t, *J* = 7.6 Hz, 2H), 7.34 (t, *J* = 7.3 Hz, 1H), 7.01 (d, *J* = 8.6 Hz, 1H), 5.42 (s, 2H); ^{13}C NMR (176 MHz, DMSO): δ 163.04, 145.01, 138.10, 137.73, 136.36, 129.42, 128.86, 128.35, 128.23, 127.36, 111.43, 67.52; HRMS (ESI) calcd for $[C_{30}H_{24}N_2O_2 + H]^+$ *m*/*z*, 445.1911; found, 445.1915.

*2,5-Bis(6-(benzyloxy)pyridin-3-yl)pyridine **3**′*. Pale-yellow solid (0.58 g, 1.3 mmol, 81%). mp 169 °C; FTIR ν 3061, 3034, 2947, 1602, 1568, 1504, 1468, 1452, 1406,1344, 1308, 1283, 1246, 1134, 1006, 983, 921, 875, 825, 773, 743, 734, 703, 694 cm^{-1}; ^{1}H NMR (700 MHz, DMSO): δ 8.98 (dd, *J* = 30.1, 2.3 Hz, 2H), 8.64 (d, *J* = 2.4 Hz, 1H), 8.47 (dd, *J* = 8.6, 2.4 Hz, 1H), 8.19 (td, *J* = 8.1, 2.5 Hz, 2H), 8.08 (d, *J* = 8.3 Hz, 1H), 7.51−7.46 (m, 4H), 7.40 (t, *J* = 7.5 Hz, 4H), 7.34 (t, *J* = 7.3 Hz, 2H), 7.08−6.98 (m, 2H), 5.44 (d, *J* = 6.1 Hz, 4H); ^{13}C NMR (176 MHz, DMSO): δ 164.01, 163.39, 153.04, 147.68, 145.75, 124.32, 138.19, 137.83, 137.66, 137.61, 135.21, 128.86, 128.43, 128.36, 128.28, 128.25, 126.70, 120.16, 111.61, 111.37,

https://doi.org/10.1021/acsomega.1c05561
ACS Omega 2021, 6, 35649−35656

67.70, 67.58; HRMS (ESI) calcd for $[C_{29}H_{23}N_3O_2 + H]^+$ *m/z*, 446.1863; found, 446.1853.

*2,5-Bis(6-(benzyloxy)pyridin-3-yl)pyrazine **4′***. Yellow solid (0.56 g, 1.26 mmol, 79%). mp 208 °C; FTIR *ν* 3068, 3030, 2874, 1601, 1566, 1517, 1495, 1467, 1452, 1395, 1360, 1308, 1269, 1236, 1185, 1157, 1111, 1076, 1021, 936, 919, 877, 848, 831, 756, 726, 706, 689 cm−1; 1H NMR (700 MHz, DMSO): *δ* 9.33 (d, *J* = 1.9 Hz, 1H), 9.01 (s, 1H), 8.50 (dt, *J* = 8.7, 2.3 Hz, 1H), 7.49 (d, *J* = 7.6 Hz, 2H), 7.41 (t, *J* = 7.5 Hz, 2H), 7.35 (t, *J* = 7.0 Hz, 1H), 7.08 (dd, *J* = 8.6, 1.6 Hz, 1H), 5.46 (s, 2H); 13C NMR (176 MHz, DMSO): *δ* 164.41, 148.05, 145.99, 141.20, 137.84, 137.50, 128.88, 128.44, 128.32, 126.01, 111.74, 67.81; HRMS (ESI) calcd for $[C_{28}H_{22}N_4O_2 + H]^+$ *m/z*, 447.1816; found, 447.1831.

General Method to Prepare 2−4. Purified and dried 2-(benzyloxy)-5-(4-(6-(benzyloxy)pyridin-3-yl)phenyl)pyridine **2′** (0.5 g, 1.13 mmol), 2,5-bis(6-(benzyloxy)pyridin-3-yl)-pyridine **3′** (0.45 g, 1.01 mmol), and 2,5-bis(6-(benzyloxy)-pyridin-3-yl)pyrazine **4′** (0.45 g, 1.0 mmol) were taken in a flask containing methanol (45 mL). Concentrated hydrochloric acid (15 mL) was added dropwise to the above solution, making the solution clear. The mixtures were heated to reflux overnight and then cooled to room temperature and neutralized using a saturated solution of sodium bicarbonate until pH = 7. The resulting precipitates were washed in water, filtered, and dried to give **2−4**, respectively.

*5-(4-(1,6-Dihydro-6-oxopyridin-3-yl)phenyl)pyridin-2(1H)-one **2***. Colourless solid (0.28 g, 1.07 mmol, 95%). mp 338 °C; FTIR *ν* 3271, 3122, 3027, 2948, 2829, 1645, 1609, 1548, 1514, 1463, 1434, 1342, 1297, 1239, 1143, 1014, 989, 928, 908, 824, 754, 723, 662 cm^{-1}; ^{1}H NMR (700 MHz, DMSO): *δ* 11.86 (s, 1H), 7.89 (ddd, *J* = 21.8, 9.5, 2.7 Hz, 1H), 7.75 (d, *J* = 8.4 Hz, 1H), 7.70−7.59 (m, 2H), 6.46 (dd, *J* = 13.1, 9.5 Hz, 1H); ^{13}C NMR (176 MHz, DMSO): *δ* 162.21, 140.31, 138.16, 135.65, 134.87, 127.34, 126.17, 126.08; HRMS (ESI) calcd for $[C_{16}H_{12}N_2O_2 + H]^+$ *m/z*, 265.0972; found, 265.0973.

*5-(5-(1,6-Dihydro-6-oxopyridin-3-yl)pyridin-2-yl)pyridin-2(1H)-one **3***. Yellow solid (0.25 g, 0.92 mmol, 92%). mp 330 °C; FTIR *ν* 3271, 3132, 2953, 2830, 1650, 1614, 1549, 1489, 1469, 1432, 1392, 1310, 1259, 1223, 1143, 996, 882, 821, 768, 668 cm^{-1}; ^{1}H NMR (700 MHz, DMSO): *δ* 11.95 (s, 2H), 8.80 (d, *J* = 2.1 Hz, 1H), 8.22 (dd, *J* = 9.6, 2.7 Hz, 1H), 8.17 (d, *J* = 2.4 Hz, 1H), 8.01 (dd, *J* = 8.4, 2.4 Hz, 1H), 7.92 (dd, *J* = 9.5, 2.7 Hz, 1H), 7.88−7.82 (m, 2H), 6.50−6.42 (m, 2H); ^{13}C NMR (176 MHz, DMSO): *δ* 162.54, 162.21, 151.62, 146.39, 140.06, 139.23, 134.52, 133.95, 133.67, 129.99, 120.76, 120.32, 118.63, 117.05, 115.02; HRMS (ESI) calcd for $[C_{15}H_{11}N_3O_2 + H]^+$ *m/z*, 266.0924; found, 266.0922.

*5-(5-(1,6-Dihydro-6-oxopyridin-3-yl)pyrazin-2-yl)pyridin-2(1H)-one **4***. Orange solid (0.24 g, 0.9 mmol, 90%). mp 341 °C; FTIR *ν* 3126, 3046, 2690, 1685, 1645, 1559, 1498, 1471, 1432, 1383, 1333, 1277, 1252, 1239, 1195, 1161, 1078, 1018, 992, 973, 888, 839, 673 cm^{-1}; ^{1}H NMR (700 MHz, TFA-d): *δ* 9.43 (s, 1H), 8.87 (s, 1H), 8.79 (d, *J* = 8.9 Hz, 1H), 7.46 (d, *J* = 9.1 Hz, 1H); ^{13}C NMR (176 MHz, TFA-d): *δ* 163.26, 146.42, 14.06, 140.26, 136.40, 120.80, 117.73; HRMS (ESI) calcd for $[C_{14}H_{10}N_4O_2 + H]^+$ *m/z*, 267.0877; found, 267.0882.

Crystallization Conditions for 2−4. All compounds were crystallized by slow diffusion. Compound **2** (10 mg) was dissolved in TFA (2 mL), and chloroform was diffused to the solution mixture. Compound **3** (10 mg) was dissolved in DMSO (3 mL), and water was diffused to the solution mixture. The same crystallization method as **2** has been used to grow the crystal salt of **4**, excepting that chloroform has been replaced with water.

■ ASSOCIATED CONTENT

Supporting Information

The Supporting Information is available free of charge at https://pubs.acs.org/doi/10.1021/acsomega.1c05561.

NMR, IR, and XRD data (PDF)

Crystallographic data of compounds (CIF)

Crystallographic data of compounds (CIF)

Crystallographic data of compounds (CIF)

■ AUTHOR INFORMATION

Corresponding Author

Adam Duong − *Département de Chimie, Biochimie et Physique and Institut de Recherche sur l'Hydrogène, Université du Québec à Trois-Rivières, Trois-Rivières, Québec G9A 5H7, Canada;* orcid.org/0000-0002-4927-3603; Email: adam.duong@uqtr.ca

Authors

Midhun Mohan − *Département de Chimie, Biochimie et Physique and Institut de Recherche sur l'Hydrogène, Université du Québec à Trois-Rivières, Trois-Rivières, Québec G9A 5H7, Canada*

Mohamed Essalhi − *Département de Chimie, Biochimie et Physique and Institut de Recherche sur l'Hydrogène, Université du Québec à Trois-Rivières, Trois-Rivières, Québec G9A 5H7, Canada*

Sarah Zaye − *Département de Chimie, Biochimie et Physique and Institut de Recherche sur l'Hydrogène, Université du Québec à Trois-Rivières, Trois-Rivières, Québec G9A 5H7, Canada*

Love Karan Rana − *Département de Chimie, Biochimie et Physique and Institut de Recherche sur l'Hydrogène, Université du Québec à Trois-Rivières, Trois-Rivières, Québec G9A 5H7, Canada*

Thierry Maris − *Département de Chimie, Université de Montréal, Montréal, Québec H3T 1J4, Canada;* orcid.org/0000-0001-9731-4046

Complete contact information is available at: https://pubs.acs.org/10.1021/acsomega.1c05561

Notes

The authors declare no competing financial interest.

■ ACKNOWLEDGMENTS

We are grateful to the Natural Sciences and Engineering Research Council of Canada (RGPIN-2015-06425), the Canadian Queen Elizabeth II Diamond Jubilee Scholarships, the *Fonds de recherche du Québec—Nature et technologies*, The Canadian Foundation for Innovation (37843), Mitacs, and the *Université du Québec à Trois-Rivières*.

■ REFERENCES

(1) Galek, P. T. A.; Chisholm, J. A.; Pidcock, E.; Wood, P. A. Hydrogen-bond coordination in organic crystal structures: statistics, predictions and applications. *Acta Crystallogr., Sect. B: Struct. Sci., Cryst. Eng. Mater.* **2014**, *70*, 91−105.

(2) Pitzer, K. S. The nature of the chemical bond and the structure of molecules and crystals: an introduction to modern structural chemistry. *J. Am. Chem. Soc.* **1960**, *82*, 4121.

(3) Zaworotko, M. J. Molecules to Crystals, Crystals to Molecules ... and Back Again? *Cryst. Growth Des.* **2007**, *7*, 4−9.
(4) Yu, Y.; Tyrikos-Ergas, T.; Zhu, Y.; Fittolani, G.; Bordoni, V.; Singhal, A.; Fair, R. J.; Grafmüller, A.; Seeberger, P. H.; Delbianco, M. Systematic Hydrogen-Bond Manipulations To Establish Polysaccharide Structure-Property Correlations. *Angew. Chem., Int. Ed.* **2019**, *58*, 13127−13132.
(5) Zhou, B.; Yan, D. Hydrogen-Bonded Two-Component Ionic Crystals Showing Enhanced Long-Lived Room-Temperature Phosphorescence via TADF-Assisted Förster Resonance Energy Transfer. *Adv. Funct. Mater.* **2019**, *29*, 1807599.
(6) Lemmerer, A.; Adsmond, D. A.; Esterhuysen, C.; Bernstein, J. Polymorphic Co-crystals from Polymorphic Co-crystal Formers: Competition between Carboxylic Acid···Pyridine and Phenol···Pyridine Hydrogen Bonds. *Cryst. Growth Des.* **2013**, *13*, 3935−3952.
(7) White, N. G.; Carta, V.; MacLachlan, M. J. Layered 2D Sheetlike Supramolecular Polymers Formed by O-H···Anion Hydrogen Bonds. *Cryst. Growth Des.* **2015**, *15*, 1540−1545.
(8) Duong, A.; Rajak, S.; Tremblay, A. A.; Maris, T.; Wuest, J. D. Molecular Organization in Crystals of Bis(diaminotriazinyl)-Substituted Derivatives of Benzene, Pyridine, and Pyrazine. *Cryst. Growth Des.* **2018**, *19*, 1299−1307.
(9) Peter, A.; Mohan, M.; Maris, T.; Wuest, J. D.; Duong, A. Comparing Crystallizations in Three Dimensions and Two Dimensions: Behavior of Isomers of [2,2′-Bipyridine]dicarbonitrile and [1,10-Phenanthroline]dicarbonitrile. *Cryst. Growth Des.* **2017**, *17*, 5242−5248.
(10) Mohan, M.; Rana, L. K.; Maris, T.; Duong, A. Intercalated 2D+2D hydrogen-bonded sheets in co-crystals of cobalt salt with 1H,1′H-[3,3′] bipyridinyl-6,6′-dione. *Can. J. Chem.* **2020**, *98*, 347−351.
(11) Su, Z.; Zhang, R.; Yan, X.-Y.; Guo, Q.-Y.; Huang, J.; Shan, W.; Liu, Y.; Liu, T.; Huang, M.; Cheng, S. Z. D. The role of architectural engineering in macromolecular self-assemblies via non-covalent interactions: A molecular LEGO approach. *Prog. Polym. Sci.* **2020**, *103*, 101230.
(12) Rawson, J. M.; Winpenny, R. E. P. The coordination chemistry of 2-pyridone and its derivatives. *Coord. Chem. Rev.* **1995**, *139*, 313−374.
(13) Mohan, M.; Maris, T.; Duong, A. Building coordination polymers using dipyridone ligands. *CrystEngComm* **2020**, *22*, 441−447.
(14) Michelson, A. Z.; Petronico, A.; Lee, J. K. 2-Pyridone and derivatives: gas-phase acidity, proton affinity, tautomer preference, and leaving group ability. *J. Org. Chem.* **2012**, *77*, 1623−1631.
(15) Mata, S.; Cortijo, V.; Caminati, W.; Alonso, J. L.; Sanz, M. E.; López, J. C.; Blanco, S. Tautomerism and microsolvation in 2-hydroxypyridine/2-pyridone. *J. Phys. Chem. A* **2010**, *114*, 11393−11398.
(16) Almlöf, J.; Kvick, Å.; Olovsson, I. Hydrogen bond studies. XLVII. The crystal structure of the intermolecular complex 2-pyridone:6-chloro-2-hydroxypyridine. *Acta Crystallogr., Sect. B: Struct. Sci., Cryst. Eng. Mater.* **1971**, *27*, 1201−1208.
(17) Zhang, G.; Rominger, F.; Mastalerz, M. Hydrogen-bonded chains and networks of triptycene-based triboronic acid and tripyridinone. *Cryst. Growth Des.* **2016**, *16*, 5542−5548.
(18) Saied, O.; Maris, T.; Wuest, J. D. Deformation of porous molecular networks induced by the exchange of guests in single crystals. *J. Am. Chem. Soc.* **2003**, *125*, 14956−14957.
(19) Owen, G. R.; Haddow, M. F. catena-Poly[[[bis(2-pyridone-κO)sodium]-di-μ-2-pyridone-κ4O:O] tetrafluoroborate]. *Acta Crystallogr., Sect. E: Struct. Rep. Online* **2007**, *63*, m83−m85.
(20) Malek, N.; Maris, T.; Perron, M.-È.; Wuest, J. D. Molecular Tectonics: Porous Cleavable Networks Constructed by Dipole-Directed Stacking of Hydrogen-Bonded Sheets. *Angew. Chem., Int. Ed.* **2005**, *44*, 4021−4025.
(21) Simard, M.; Su, D.; Wuest, J. D. Use of hydrogen bonds to control molecular aggregation. Self-assembly of three-dimensional networks with large chambers. *J. Am. Chem. Soc.* **1991**, *113*, 4696−4698.
(22) Etter, M. C.; MacDonald, J. C.; Bernstein, J. Graph-Set Analysis of Hydrogen-Bond Patterns in Organic Crystals. *Acta Crystallogr., Sect. B: Struct. Sci.* **1990**, *46*, 256−262.
(23) Reedijk, J. The ligand properties of hydroxypyridines: Part I. Hexakis(2-pyridone) metal perchlorates and tetrafluoroborates. *Recl. Trav. Chim. Pays-Bas* **1969**, *88*, 1139−1155.
(24) Deng, H.; Grunder, S.; Cordova, K. E.; Valente, C.; Furukawa, H.; Hmadeh, M.; Gándara, F.; Whalley, A. C.; Liu, Z.; Asahina, S.; Kazumori, H.; O'Keeffe, M.; Terasaki, O.; Stoddart, J. F.; Yaghi, O. M. Large-pore apertures in a series of metal-organic frameworks. *Science* **2012**, *336*, 1018−1023.
(25) Ding, M.; Cai, X.; Jiang, H.-L. Improving MOF stability: approaches and applications. *Chem. Sci.* **2019**, *10*, 10209−10230.
(26) Ueda, M.; Mochida, T.; Mori, H. Pyridone derivatives carrying radical moieties: Hydrogen-bonded structures, magnetic properties, and metal coordination. *Polyhedron* **2013**, *52*, 755−760.
(27) Devendar, P.; Qu, R.-Y.; Kang, W.-M.; He, B.; Yang, G.-F. Palladium-catalyzed cross-coupling reactions: a powerful tool for the synthesis of agrochemicals. *J. Agric. Food Chem.* **2018**, *66*, 8914−8934.
(28) Kotha, S.; Lahiri, K.; Dhurke, K. Recent applications of the Suzuki−Miyaura cross-coupling reaction in organic synthesis. *Tetrahedron* **2002**, *58*, 9633.
(29) Spackman, P. R.; Turner, M. J.; McKinnon, J. J.; Wolff, S. K.; Grimwood, D. J.; Jayatilaka, D.; Spackman, M. A. CrystalExplorer: a program for Hirshfeld surface analysis, visualization and quantitative analysis of molecular crystals. *J. Appl. Crystallogr.* **2021**, *54*, 1006−1011.
(30) Sheldrick, G. M. SHELXT- Integrated space-group and crystal-structure determination. *Acta Crystallogr.* **2015**, *71*, 3−8.
(31) Sheldrick, G. M. Crystal structure refinement with SHELXL. *Acta Crystallogr.* **2015**, *71*, 3−8.